Draft version March 18, 2015
Preprint typeset using LaTeX style emulateapj v. 12/16/11

TITULO

Maria Camila Remolina-Gutierrez, Jaime E. Forero-Romero & Juan N. Garavito-Camargo
Departamento de Física, Universidad de los Andes, Cra. 1 No. 18A-10, Edificio Ip, Bogotá, Colombia

Julian Mejía
Chile

Alvaro Orsi
Spain
Draft version March 18, 2015

ABSTRACT

MISSING: The abstract

Subject headings: Galaxies: high-redshift, Lyman Alpha Emission, Galaxy Rotation, Galaxy Outflows
....MISSING....

1. INTRODUCTION

Partridge & Peebles (1967) predicted a population of galaxies with a strong Lyman Alpha (Ly-α) emission, nowadays galaxies selected using the Ly-α line are known as Lyman Alpha Emitters (LAEs). Since the first observed LAE by Djorgovski & Thompson (1992) different teams have observed several LAEs Rhoads et al. (2000); Gawiser et al. (2007); Koehler et al. (2007); Ouchi et al. (2008); Yamada et al. (2012); Schenker et al. (2012); Kulas et al. (2012); Yamada et al. (2012); Chonis et al. (2013); Finkelstein et al. (2013); Östlin et al. (2014) with the aim of exploring the extragalactic Universe. Specially at $z >= 2$ since it is when the line is redshifted into the optical regime. With the outcoming of new and powerful telescopes such as the James Webb Space Telescope new LAEs are going to be discovered with a better resolution and at higher redshifts.

This observations have a direct impact in studying the reionization epoch see Dijkstra (2014) fore more details and references in within, properties of the interstellar medium (ISM) and the intergalactic medium (IGM) (Behrens & Niemeyer 2013) (Dijkstra & Kramer 2012), constraining star formation rates of high redshift galaxies, understanding galaxy luminosity functions Gronke et al. (2015) and studying the large scale structure of the Universe. In all of this studies is required an understanding of the processes that model the morphology and the radiate transfer process behind of the Ly-α line.

To fully understand the observed spectra of the LAEs this galaxies must be modeled. However the resonant nature of the line makes this a challenging task. Analytical solutions for the outcoming spectra in simple ISM static geometries have been derived Adams (1972); Harrington (1973); Neufeld (1990); Dijkstra et al. (2006). Radiative transfer codes (Dijkstra & Kramer 2012; Laursen et al. 2009; Verhamme et al. 2006; Forero-Romero et al. 2011) have been developed in order to understand the effect of the gas kinematics in the Ly-α line, special attention have been devoted to the effects of clumpy media (Hansen & Oh 2006) and expanding/contracting shell/spherical geometries started to be studied (Ahn et al. 2003; Verhamme et al. 2006; Dijkstra et al. 2006). Recently Garavito-Camargo et al. (2014) have studied in detail the effect of rotation on the lyman alpha line. Hydrodynamic simulations have studied the outcomming spectra of LAEs in large scale simulations Forero-Romero et al. (2012), Recently Monte Carlo codes have been used in hydrodynamic simulations to study in detail individual galaxies (Laursen et al. 2009; Barnes et al. 2011; Verhamme et al. 2012; Yajima et al. 2012).

Especial attention have been devoted to model the presence of outflows in the galaxy, motivates by previous observational studies*. Outflows are a consequence of the interstellar medium (ISM) being ejected from the galaxy due to supernova explosions. Here different models have attempt to simulate more realistic situations involving shell models and cavities. (Behrens et al. 2014).

Despite the fact that outflows have been broadly studied rotation should also be present in this galaxies. The joint effect of the two above properties should have a direct effect on the morphology of the Ly-α line.

Study this effect is the main motivation of this paper in which we combine the effect of rotation followed by an outflow. We proposed a simplified model in which the galaxy is modeled as an sphere undergoing solid-body rotation, with an homogeneous mixture of dust and hydrogen at a constant temperature.

The solid-body rotation does not induce any spatial anisotropy in the integrated line flux, the escape fraction or in the average number of scatterings. This symmetry allows to the creation of an analytic approximation for the galaxy spectrum proposed, see Garavito-Camargo et al. (2014) for details. In this model the optical depth τ_H, the rotation velocity V_{max} and the inclination angle

mc.remolina197@uniandes.edu.co
je.forero@uniandes.edu.co
jn.garavito57@uniandes.edu.co

θ are free parameters.

The outcoming spectra of the rotating galaxy is then affected by a symmetric thin shell of expanding gas at a constant velocity following the model proposed by Verhamme et al. (2014); Orsi et al. (2012).

This paper is structured as follows. In §2 we explain in detail the model of rotation and outflow that we use as well and our joint model (Rotation & Outflow). In §3 we present the results of our model. In §4 we compare our results with recent observations of LAEs with special attention of those morphologies that present features of galaxy rotation and outflows. In the latest section we present our conclusions.

2. THEORETICAL BACKGROUND

In this section we describe the two different models that together are used to reproduce a real and consistent Ly-α profile. The first one is a rotation model for the galaxy and the second is a thin shell model for the outflow.

2.1. *Rotation Model*

We use the simplified rotation model developed by (Garavito-Camargo et al. 2014) in which a rotating galaxy is modeled as a solid rotating sphere, with a homogeneous mixture of hydrogen and dust. Photons can be initially at the center or can be homogeneously distributed inside the sphere. The equations governing this solid-body rotation sphere in which the axis of rotation is defined to be align with the z-axis are:

$$v_x = -\frac{y}{R} V_{\max}, \tag{1}$$

$$v_y = \frac{x}{R} V_{\max}, \tag{2}$$

$$v_z = 0, \tag{3}$$

Where R is the radius of the sphere and $V_{\max}$ is the linear velocity at the sphere's surface. The minus/plus sign in the x/y-component of the velocity indicates the direction of rotation. In this case we take the angular velocity in the same direction as the $\hat{k}$ unit vector.

In this work we use the analytical expression for rotation derived in (Garavito-Camargo et al. 2014) where a rotating sphere can be seen as a static sphere in the laboratory frame with a bulk velocity difference in each surface element with respect to a distant observer. With the previous analysis the outcoming spectra can be expressed as:

$$J(x,i) \approx 2\pi \int_0^R db\, b \int_0^{2\pi} d\phi\, J(x,b,\phi,i), \tag{4}$$

Where $J(x,b,\phi,i)$ is the spectrum of the flux emerging from the surface at point (b,ϕ) and is expressed as:

$$J(x,b,\phi,i) = \frac{\sqrt{\pi}}{\sqrt{24} a\tau_0} \left(\frac{(x-x_{\rm b})^2}{1+\cosh\left[\sqrt{\frac{2\pi^3}{27}} \frac{|(x-x_{\rm b})^3|}{a\tau_0}\right]} \right) \tag{5}$$

2.2. *Outflow Model: Thin Shell*

We use an outflow model that follows the characteristics put described in (Verhamme et al. 2006) with the code presented in(Orsi et al. 2012). The outflow consists of an isothermal, spherical flow expanding at constant velocity v_{out} . The outflow is empty inside the shell's inner radius R_{in} and reaches out to an external radius R_{out}. The relationship between these two radii is parameterized by $R_{in} = f_{th} R_{out}$, with $f_{th} = 0.9$ as the fiducial value. The temperature of the medium is assumed constant and equal to $T = 10^4 K$ which sets the velocity dispersion of Maxwell-Boltzmann distributions to $v_{\rm th} = 12.84\,{\rm km\ s^{-1}}$.

The gas has an homogeneous Hydrogen number density inside the flow. The total mass inside the shell is parameterized by its column density

$$N_H = \frac{X_H M_{shell}}{4\pi m_H R^2{}_{out}}, \tag{6}$$

where M_{shell} is the outflow mass, m_H is the mass of the hydrogen atom and $X_H = 0.74$ is the fraction of hydrogen in the cold gas.

The outflow also includes dust homogeneously mixed with the gas. The dust optical depth τ_d is parameterized by the metallicity of the cold gas $\langle Z_{cold} \rangle$:

$$\tau_d ???? \langle Z_{cold} \rangle \tag{7}$$

2.3. *Joint Model*

The joint model consists of combining the two models that were just explained. A rotating spherical galaxy is placed at the center with a thin shell outflow surrounding it as seen in Fig. 1. What happens is that the photons that escaped the galaxy enter now into the outflow with the same radial direction that they came out with. At the end only a fraction of those manage to get out of the outflow and their wavelengths are measured to find the final spectrum.

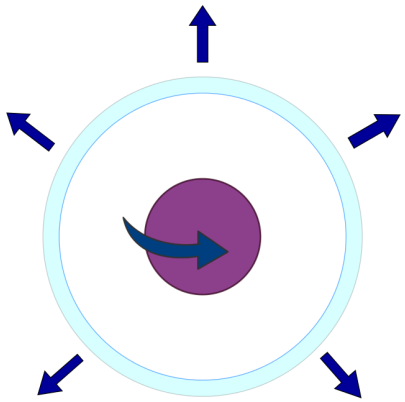

FIG. 1.— **Model:** A central rotating galaxy surrounded by an expanding thin shell outflow.

In order to simulate all the possible cases we set some key parameters for the program to vary, and some others fixed which are defined by the characteristics of LAEs. This are chosen as follows.

2.3.1. *Galaxy Parameters*

Our aim is to provide a realistic baseline to compare against observations of LAES at $z \sim 3$. It has been found by analysis of the abundance and angular correlation function that LAES reside in DM halos of masses in the range $10^{10} - 10^{11} M_\odot$ Walker-Soler et al. (2012). This mass range corresponds to maximum circular velocities in the range $60 - 125\,\mathrm{km\ s^{-1}}$ and a median halo scale radius of 15kpc. [1].

These galaxies have gas fractions close to 20% (Narayanan et al. 2012). We approximate that the hydrogen content is 20% the total baryonic content from the cosmological baryon to dark matter abundances $\Omega_b/\Omega_{dm} = 0.1825$ (Planck Collaboration et al. 2015), multiplied by a primordial Hydrogen fraction of 0.75. All these considerations gives us hydrogen masses in the range $2.7 \times 10^8 - 2.7 \times 10^9 M_\odot$.

These choices give us a range for the number density of Hydrogen atoms of $4 \times 10^{-4} - 4 \times 10^{-3}$ atoms cm^{-3}. With a Lyman-α cross section at the line center of $\sigma_H = 1.0 \times 10^{-14}$ cm^2 we finally obtain that the optical depth from the cloud's center should be in the range $\tau = 2 \times 10^5 - 2 \times 10^6$.

From these constraints we chose to model two kinds of central galaxies in the extremes of these distributions. The first has $\tau = 2 \times 10^5$ and a raotational velocity of $60\,\mathrm{km\ s^{-1}}$. The second has $\tau = 2 \times 10^6$ and a rotational velocity of $125\,\mathrm{km\ s^{-1}}$.

2.3.2. *Fixed Parameters*

For the first stage there are two fixed parameters: the optical depth $\tau = 10^8$ and the galaxy rotation velocity $v_{gal} = 100$ km s^{-1}. For the second stage there is one fixed parameter: the metallicity of the outflow $Z = -4.0$. This 3 fixed values are selected because the characteristics of observed LAEs, especially their low mass and their highest star formation rate of all.

2.3.3. *Free Parameters*

We have then 3 parameters left that are going to vary along a wide range. These are: the galaxy viewing angle θ_{gal} , the hydrogen column density n_H and the outflow expanding velocity v_{out} .

θ_{gal} covers 3 different angles: 0°, 45° and 90°. $\log n_H$ takes 41 different values from 20.0 to 22.5. And v_{out} covers 5 equidistant velocities from 100 km s^{-1} to 500 km s^{-1}. The permutations of these three are analyzed in section 3.

3. RESULTS

The results of this project consist of emulating a LAE spectrum basing on its physical characteristics defined by the 3 free parameters we stated before. When defined the combination of those three.

MISSING:
- What are the compact results.
- Not a physical analysis yet.
- Write better (prettier)

---

[1] These results were found using the N-body data available in www.cosmosim.org

In the following subsection each free parameter is explained deeper.

3.1. *Influences of the Free Parameters*

In order to study the influence of each of the three free parameters, we fix two of them and see how the final spectrum varies along the other one left. In each case we will state these changes.

3.1.1. *Influence of the Galaxy Viewing Angle: θ_{gal}*

If one sets fixed outflow v_{out} and $\log n_H$ in each case the viewing angle has the same effect: it increases proportionally the intensity. However this change is not that significant. The resulting spectra are completely the same, but enlarged vertically by a small factor. Fig. 2 helps visualize this effect in a better way.

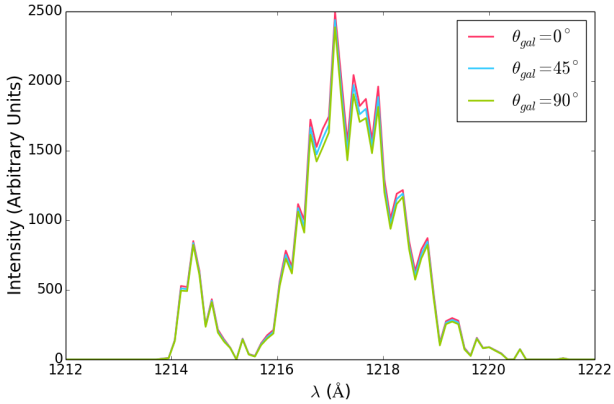

FIG. 2.— **Influence of Galaxy Viewing Angle:** The values of the fixed parameters are $v_{out} = 100$ km s^{-1} and $\log n_H = 21.3125$. The 3 possible angles are shown in the plot with different colors. The increase is visible as well as its small enlargement factor.

3.1.2. *Influence of the Outflow Hydrogen Column Density: $\log n_H$*

The effect of the $\log n_H$ is the creation of 2 peaks: the left one very thin, tall and pronounced, and the right one very wide, small and soften. When the *lognH* is increased, the left peak starts to decrease while mixing with the right one, decreasing their height ratio until the left peak completely disappears. The resulting spectrum, with high column density, is a wide single mountain with intensity significantly less than at the beginning. Fig. 3 helps visualize this effect in a better way.

3.1.3. *Influence of the Outflow Expanding Velocity: v_{out}*

The effect of this parameter consists in a shift of the initial spectrum in the column density. The more v_{out} the outflow has, the more the spectrum simulates the previous velocity but with a greater $\log n_H$. If one compares with Fig. 3 the similarities are really clear.

4. DISCUSSION

MISSING:

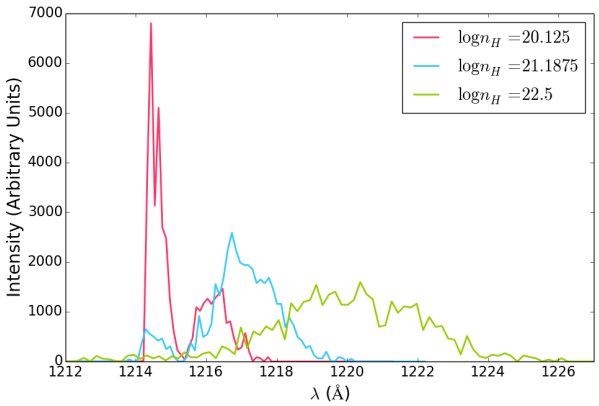

FIG. 3.— **Influence of Outflow Hydrogen Column Density:** The values of the fixed parameters are $v_{out} = 100$ km s^{-1}and $\theta_{gal} = 90°$. There are three stages of the $\log n_H$ value shown: initial, intermediate and final, with the values shown on the plot.

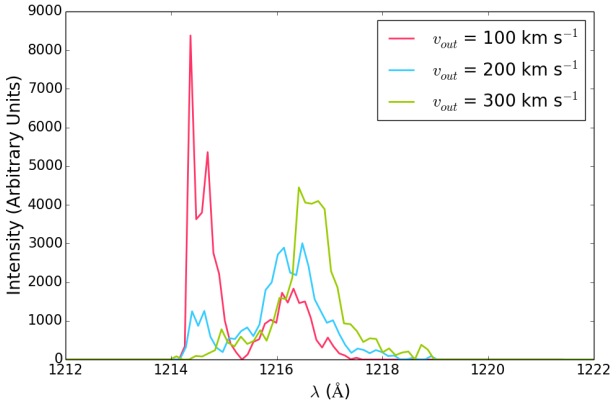

FIG. 4.— **Influence of Outflow Expanding Velocity:** The values of the fixed parameters are $\log n_H = 20.0625$ and $\theta_{gal} = 90°$. If one increases $\log n_H$ for an outflow with $v_{out} = 100$ km s^{-1}it will create similar spectra to these in certain points.

- Comparison with some other result (probably observations).
- Why is this result useful?
- What possible implications can this model have?

Ideas:

The decrease of the intensity while increasing the column density is caused because the second is proportional to the absorption of light in the gas. The more $\log n_H$, the less photons get out of the outflow.

5. CONCLUSIONS

Here goes the conclusions....

ACKNOWLEDGMENTS

We acknowledge Alvaro Orsi and Julian Mejia for collaborating with us offering their time, advice and especially data. We used their outflow simulations in order to get our results.

The data, source code and instructions to replicate the results of this paper can be found here `https://github.com/mariacamilaremolinagutierrez/LymanAlpha/`. Most of our code benefits from the work of the IPython and Matplotlib communities (Pérez & Granger 2007; Hunter 2007).

MISSING:
- More acknowledgments.

REFERENCES

Adams, T. F. 1972, ApJ, 174, 439
Ahn, S.-H., Lee, H.-W., & Lee, H. M. 2003, MNRAS, 340, 863
Barnes, L. A., Haehnelt, M. G., Tescari, E., & Viel, M. 2011, MNRAS, 416, 1723
Behrens, C., Dijkstra, M., & Niemeyer, J. C. 2014, A&A, 563, A77
Behrens, C., & Niemeyer, J. 2013, A&A, 556, A5
Chonis, T. S., Blanc, G. A., Hill, G. J., Adams, J. J., Finkelstein, S. L., Gebhardt, K., Kollmeier, J. A., Ciardullo, R., Drory, N., Gronwall, C., Hagen, A., Overzier, R. A., Song, M., & Zeimann, G. R. 2013, ApJ, 775, 99
Dijkstra, M. 2014, ArXiv e-prints, arXiv:1406.7292
Dijkstra, M., Haiman, Z., & Spaans, M. 2006, ApJ, 649, 14
Dijkstra, M., & Kramer, R. 2012, MNRAS, 424, 1672
Djorgovski, S., & Thompson, D. J. 1992, in IAU Symposium, Vol. 149, The Stellar Populations of Galaxies, ed. B. Barbuy & A. Renzini, 337
Finkelstein, S. L., Papovich, C., Dickinson, M., Song, M., Tilvi, V., Koekemoer, a. M., Finkelstein, K. D., Mobasher, B., Ferguson, H. C., Giavalisco, M., Reddy, N., Ashby, M. L. N., Dekel, a., Fazio, G. G., Fontana, a., Grogin, N. a., Huang, J.-S., Kocevski, D., Rafelski, M., Weiner, B. J., & Willner, S. P. 2013, Nature, 502, 524
Forero-Romero, J. E., Yepes, G., Gottlöber, S., Knollmann, S. R., Cuesta, A. J., & Prada, F. 2011, MNRAS, 415, 3666
Forero-Romero, J. E., Yepes, G., Gottlöber, S., & Prada, F. 2012, MNRAS, 419, 952
Garavito-Camargo, J. N., Forero-Romero, J. E., & Dijkstra, M. 2014, ApJ, 795, 120
Gawiser, E., Francke, H., Lai, K., Schawinski, K., Gronwall, C., Ciardullo, R., Quadri, R., Orsi, A., Barrientos, L. F., Blanc, G. A., Fazio, G., & Feldmeier, J. J. 2007, ApJ, 671, 278
Gronke, M., Dijkstra, M., Trenti, M., & Wyithe, S. 2015, ArXiv e-prints
Hansen, M., & Oh, S. P. 2006, MNRAS, 367, 979
Harrington, J. P. 1973, MNRAS, 162, 43
Hunter, J. D. 2007, Computing In Science & Engineering, 9, 90
Koehler, R. S., Schuecker, P., & Gebhardt, K. 2007, A&A, 462, 7

Kulas, K. R., Shapley, A. E., Kollmeier, J. A., Zheng, Z., Steidel, C. C., & Hainline, K. N. 2012, ApJ, 745, 33
Laursen, P., Sommer-Larsen, J., & Andersen, A. C. 2009, ApJ, 704, 1640
Narayanan, D., Bothwell, M., & Davé, R. 2012, MNRAS, 426, 1178
Neufeld, D. A. 1990, ApJ, 350, 216
Orsi, A., Lacey, C. G., & Baugh, C. M. 2012, MNRAS, 425, 87
Östlin, G., Hayes, M., Duval, F., Sandberg, A., Rivera-Thorsen, T., Marquart, T., Orlitova, I., Adamo, A., Melinder, J., Guaita, L., Atek, H., Cannon, J. M., Gruyters, P., Herenz, E. C., Kunth, D., Laursen, P., Mas-Hesse, J. M., Micheva, G., Pardy, H. O.-F. S. A., Roth, M. M., Schaerer, D., & Verhamme, A. 2014, ArXiv e-prints
Ouchi, M., Shimasaku, K., Akiyama, M., Simpson, C., Saito, T., Ueda, Y., Furusawa, H., Sekiguchi, K., Yamada, T., Kodama, T., Kashikawa, N., Okamura, S., Iye, M., Takata, T., Yoshida, M., & Yoshida, M. 2008, ApJS, 176, 301
Partridge, R. B., & Peebles, P. J. E. 1967, ApJ, 147, 868
Pérez, F., & Granger, B. E. 2007, Computing in Science and Engineering, 9, 21
Planck Collaboration, Ade, P. A. R., Aghanim, N., Arnaud, M., Ashdown, M., Aumont, J., Baccigalupi, C., Banday, A. J., Barreiro, R. B., Bartlett, J. G., & et al. 2015, ArXiv e-prints
Rhoads, J. E., Malhotra, S., Dey, A., Stern, D., Spinrad, H., & Jannuzi, B. T. 2000, ApJ, 545, L85
Schenker, M. A., Stark, D. P., Ellis, R. S., Robertson, B. E., Dunlop, J. S., McLure, R. J., Kneib, J.-P., & Richard, J. 2012, ApJ, 744, 179
Verhamme, A., Dubois, Y., Blaizot, J., Garel, T., Bacon, R., Devriendt, J., Guiderdoni, B., & Slyz, A. 2012, A&A, 546, A111
Verhamme, A., Orlitova, I., Schaerer, D., & Hayes, M. 2014, ArXiv e-prints
Verhamme, A., Schaerer, D., & Maselli, A. 2006, A&A, 460, 397
Walker-Soler, J. P., Gawiser, E., Bond, N. A., Padilla, N., & Francke, H. 2012, ApJ, 752, 160
Yajima, H., Li, Y., Zhu, Q., Abel, T., Gronwall, C., & Ciardullo, R. 2012, ApJ, 754, 118
Yamada, T., Nakamura, Y., Matsuda, Y., Hayashino, T., Yamauchi, R., Morimoto, N., Kousai, K., & Umemura, M. 2012, AJ, 143, 79